Ultrashort Pulse Decomposition in a Turn of a Meander Microstrip Line with Two Passive Conductors

Konstantin P. Malygin, Alexander V. Nosov, Roman S. Surovtsev

Abstract – **The paper considers decomposition of an ultrashort pulse in a turn of a meander microstrip line with two passive conductors into a sequence of pulses of lower amplitude. Two circuit diagrams were discussed, differing in the location of the connection of half turns. Various boundary conditions (open circuit, short circuit and 50 Ω) of the ends of passive conductors were investigated and the optimal ones were selected according to the criterion of the minimum amplitude at the end of the line. The analysis of the influence of the geometric parameters of the line on the amplitude of the output signal was carried out. We found the optimal parameters of the structures, which ensure the decomposition of the ultrashort pulse and the minimization of its amplitude. Based on the simulation results, we obtained the attenuation of an ultrashort pulse (relative to half of the e.m.f.) in the first structure of 6.4 times, and in the second – of 10.6 times. In addition, we determined the delays of each pulse and formulated the conditions the fulfilment of which allows for the decomposition of an ultrashort pulse into 11 pulses of lower amplitude.**

Keywords – **Ultrashort pulse, Odd mode, Even mode, Additional pulse, Pulse decomposition, Protective device.**

I. INTRODUCTION

The problem of electronic equipment (EE) protection is relevant today. The influence of natural and intentional electromagnetic interference (EMI) is dangerous for critical EE without any adequate protection [1]. The big concern today is the possibility of using EMI generators for terrorist purposes for disrupting or disabling (electromagnetic terrorism) important objects of modern society, for example, objects of the fuel and energy complex [2]. A number of such cases are known and reported in different countries of the world [3]. The most dangerous are ultrashort pulses (USP) of the nanosecond and subnanosecond ranges because of the high power and short rise time [4].

There are many approaches to protection against USPs [5–7]. Each of them has its own drawbacks, the main ones of which can be low power and speed, as well as limited-service life [5]. For example, the efficiency of filters based on lumped elements can be reduced by the appearance of parasitic capacitance of the inductor at high frequencies and a high probability of penetration of ultra-wideband signals or disturbances at resonant frequencies [6]. Capacitors are susceptible to electrical breakdown: being exposed to a strong electric field the dielectric between the plates loses its isolation properties and begins to conduct the current [7]. Therefore, the search for new alternative protection devices is relevant. For example, devices protecting against USPs and based on printed lines and signal filtering in the frequency band are widely studied [8–13]. Noteworthy is the approach to the EE protection against USPs proposed by the authors and based on USP attenuation in meander lines due to modal decomposition [14]. One of its advantages is that to provide USP protection, it is not necessary to have a protection device as such: meander lines which are already available on the PCB can be used instead. The essence of the approach is to decompose the USP into a sequence of pulses of lower amplitudes, for example, in a meander microstrip line (MSL) into crosstalk, odd and even mode pulses; the USP attenuation can be reach 2.4 times. However, such USP attenuation is not sufficient and, in this regard, it is necessary to improve this approach. An increase of attenuation can be achieved with an increase of the number of decomposition pulses, for example, by adding additional passive conductors and introducing asymmetry into the cross-section of the line, as it has been done in a related works [15,16]. This will significantly increase the USP attenuation. The purpose of this work is to investigate these possibilities.

II. INITIAL DATA FOR SIMULATION

Fig. 1 shows the cross-section of the line under investigation with two additional passive conductors and 2 circuit diagrams of the line. In the first diagram, the turn is located between the passive conductors (Fig. 1*b*), and in the second – on one side of them (Fig. 1*c*). In such a structure there are 4 modes, each of which propagates with its own per-unit-length delay (τ_1, τ_2, τ_3, τ_4). Thus, with the optimal parameters of the cross-section, at the output (nodes $V6$ for circuit diagram 1 and $V4$ for circuit diagram 2) the USP can be decomposed into 5 pulses: crosstalk pulse and 4 line mode pulses. However, with an asymmetry of the cross-section, the number of pulses increases due to the appearance of additional pulses, the number of which is determined by the number of linear combinations of the mode pulse delays, similar to [15]. Taking this into account, at the end of the turn of the meander MSL with two passive conductors, 11 main decomposition pulses of lower amplitude will be observed. Then it is possible to formulate the conditions for USP decomposition in the line under investigation into a sequence of 11 pulses. However,

Article history: Received March 10, 2022; Accepted November 02, 2022

The authors are with the Tomsk State University of Control Systems and Radioelectronics, 634050, Tomsk, Russia, E-mails: malyginkp@gmail.com, surovtsevrs@tu.tusur.ru, alexns2094@tu.tusur.ru.

first we analyze the influence of the boundary conditions on the maximum USP amplitude at the end of the line (U_{max}), as well as the influence of geometric parameters of the line at U_{max} and the delays of each pulses.

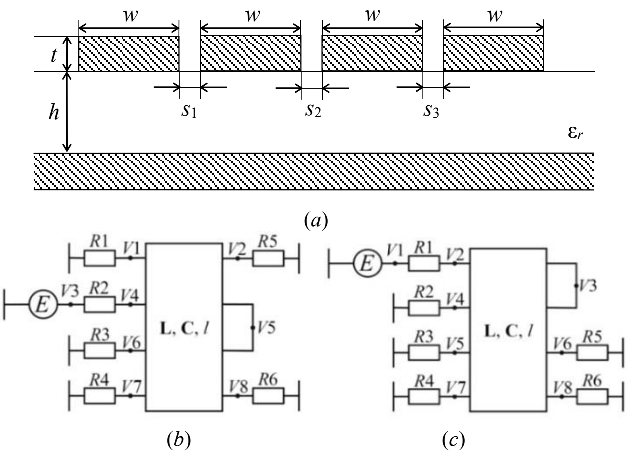

Fig. 1. Cross-section (a), circuit diagrams 1 (b) and 2 (c) of the meander MSL with two passive conductors.

III. Simulation Results

For simulation, as an excitation pulse we chose a trapezoidal pulse with an e.m.f. of 1 V, the duration of the flat top of 100 ps and the rise and fall times of 50 ps each. The internal resistances of the generator and the receiver are taken equal to 50 Ω ($R2$, $R3$ for circuit 1 and $R1$, $R2$ for circuit 2), and the boundary conditions for passive conductors ($R1$, $R5$, $R4$, $R6$ for circuit 1 and $R3$–$R6$ for circuit 2) will be chosen further from Table 1, where O means open circuit, and S – short circuit.

TABLE 1
Sets of Boundary Conditions (N) of Passive Conductors for Circuit Diagrams 1 and 2

Circuit 1	Circuit 2	1	2	3	4	5	6	7
$R1$	$R3$	O	O	S	S	S	O	50 Ω
$R5$	$R4$	O	S	O	S	S	O	50 Ω
$R4$	$R5$	O	O	S	S	O	S	50 Ω
$R6$	$R6$	O	S	O	S	O	S	50 Ω

First, the influence of the boundary conditions from Table 1 on the maximum amplitude at the end of the line was evaluated. For this, the structure under investigation was simulated with the following parameters: w=300 μm, t=18 μm, s_1=s_2=50 μm, s_3=100 μm, h=300 μm, ε_r=10, l=1 m. These parameters were obtained by heuristic search according to the criterion of USP decomposition into 11 main pulses (each pulse of the sequence arrives after the previous one ends). Simulation was performed in the TALGAT software [17, 18]. Table 2 summarizes U_{max} values at the end of each circuit (at node $V4$ for circuit 1 and at node $V6$ for circuit 2) under the boundary conditions from Table 1.

TABLE 2
Maximum USP Amplitudes at the Output of the Circuit Diagrams 1 (U_{MAX1}) and 2 (U_{MAX2}) under the Boundary

N	1	2	3	4	5	6	7
U_{max1}, V	0.182	0.191	0.118	0.201	0.136	0.119	0.109
U_{max2}, V	0.199	0.206	0.105	0.149	0.222	0.178	0.146

From Table 2 it can be seen that U_{max} in circuit 1 has a maximum value of 0.201 V for the 4th set of resistances, and the minimum is 0.109 V for set 7, and in circuit 2 – 0.222 V and 0.105 V for sets 5 and 3, respectively. Thus, for further simulation, we selected the sets of resistances that provide the minimum amplitude at the end of the line: $R1$=$R5$=$R4$=$R6$=50 Ω (N=7) for circuit 1; $R3$=$R5$=S, $R4$=$R6$=O (N=3) for circuit 2.

Then, we estimated the influence of the cross-section parameters of the turn on the maximum amplitude at the end of the meander MSL and the delay of each of the decomposition pulses. When simulating, all resistances ($R1$–$R6$) for circuits 1 and 2 are taken equal to 50 Ω. The influence of s_1, s_2, s_3, w, t and h variations on the delays of all pulses ($P2$–$P11$), except the first one, and U_{max} was analyzed at the ends of circuits 1 and 2. The values of the s_1 and s_2 parameters varied in the range of 60-100 μm with a step of 10 μm, s_3 – 110–150 μm with a step of 10 μm, w – 400-900 μm with a step of 100 μm, t – 20-60 μm with a step of 10 μm, and h – 20-900 μm with a step 100 μm. The values of ε_r and l parameters were taken as initial. Fig. 2 shows the dependences of the $P2$–$P11$ pulse delays on s_1, s_2, s_3, w, t and h coinciding for circuits 1 and 2. Fig. 3 and Fig. 4 – dependences of U_{max} at nodes $V6$ and $V4$ of circuits 1 and 2, respectively.

From Fig. 2, it can be seen that with an increase of s_1, s_2, and s_3 values, the delays of all $P2$–$P11$ pulses practically do not change. An increase of w leads to a monotonic increase of the delays of pulses $P2$–$P6$ and $P9$–$P11$, while delays of pulses $P7$ and $P8$ become closer and, with an increase of w from 700 to 900 μm, change places after intersection. An increase of t leads to a monotonic decrease of the delays of all $P2$–$P11$ pulses (with that, as the dependences move away from the horizontal axis, they change less significantly). With an increase of h, the delays of the $P2$–P11 pulses decrease; however, approaching to the horizontal axis, this decrease becomes insignificant.

From Fig. 3 it can be seen that the value of U_{max} increases monotonically with an increase of s_1 (by 26%). With an increase of s_2, the U_{max} value first slightly decreases, but, starting from the value s_2=70 μm, a monotonic increase (by 21%) is observed. A similar character is observed for the dependences of $U_{max}(s_3)$ and $U_{max}(t)$. As can be seen up to s_3=130 μm, the value of U_{max} decreases by 5%, and then, with a further increase of s_3, it increases by 9%. Then we can see, that to a value of t=40 μm, U_{max} decreases by 11%, and with a further increase of t, the value of U_{max} increases by 4%. A monotonic decrease is observed in the dependence of $U_{max}(w)$, but in the dependence of $U_{max}(h)$, quite the opposite, there is a monotonic increase. An increase of w leads to a decrease of U_{max} value by 16%, and an increase of h leads to an increase of U_{max} by 45%.

From Fig. 4 it can be seen that the value of $U_{\max}$ with a change of s_1 first decreases by 5%, and, starting from the value s_1=90 µm, increases by 3%. An increase of s_2 leads to a monotonic increase of $U_{\max}(s_2)$ dependence by 54%. An increase of s_3 leads to a slight increase of $U_{\max}$ value by 1%. An increase of w first leads to a decrease of $U_{\max}$ by 6%, and, starting from the value w=600 µm, to an abrupt increase (at w=700 µm) by 41% and a subsequent decrease by 8%. An increase of t leads to a slight change in the values of $U_{\max}$ (by 4%), and an increase of h leads to a monotonic increase of $U_{\max}$ by 35%.

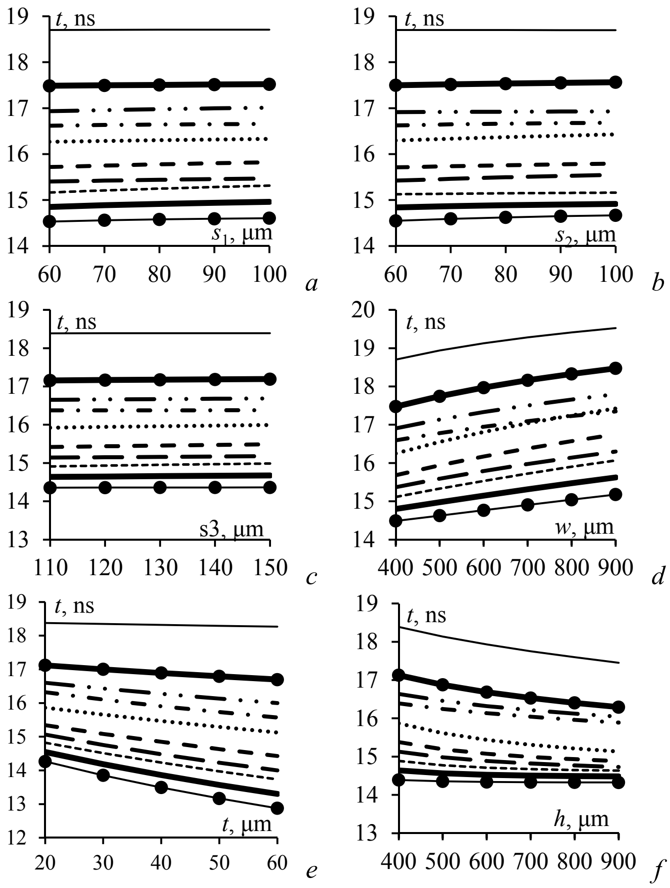

Fig. 2. Dependences of delay values of pulses $P2$ (–•–), $P3$ (Ƶ), $P4$ (---), $P5$ (– –), $P6$ (- -), $P7$ (· · · ·), $P8$ (- · -), $P9$ (– · · –), $P10$ (Ƶ •Ƶ), $P11$ (—) on s_1 (a), s_2 (b), s_3 (c), w (d), t (e) and h (f) of the meander MSL.

Taking into account the analysis results, parameters that ensure the minimum amplitude of the output signal and the decomposition of the USP into 11 pulses at the end of the turn were obtained. For the line with circuit 1 with N=7, the following parameters were obtained: w=400 µm, t=18 µm, s_1=110 µm, s_2=s_3=40 µm, h=300 µm, ε_r=25, l=1.2 m. For the line with circuit 2 with N=3, the following parameters were obtained: w=2000 µm, t=18 µm, s_1=s_2=50 µm, s_3=105 µm, h=300 µm, ε_r=20, l=1.2 m. The voltage waveforms simulated for comparison in the TALGAT and ADS software at the end of circuits 1 and 2 with the optimal parameters are shown in Fig. 5.

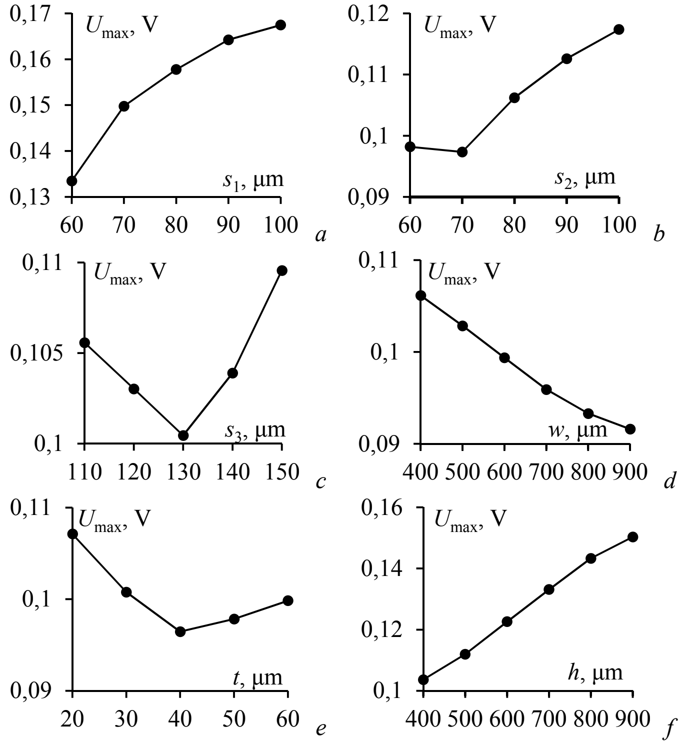

Fig. 3. Dependences of $U_{\max}$ at the end of circuit diagram 1 on w (a), s_1 (b), s_2 (c), s_3 (d), t (e) and h (f).

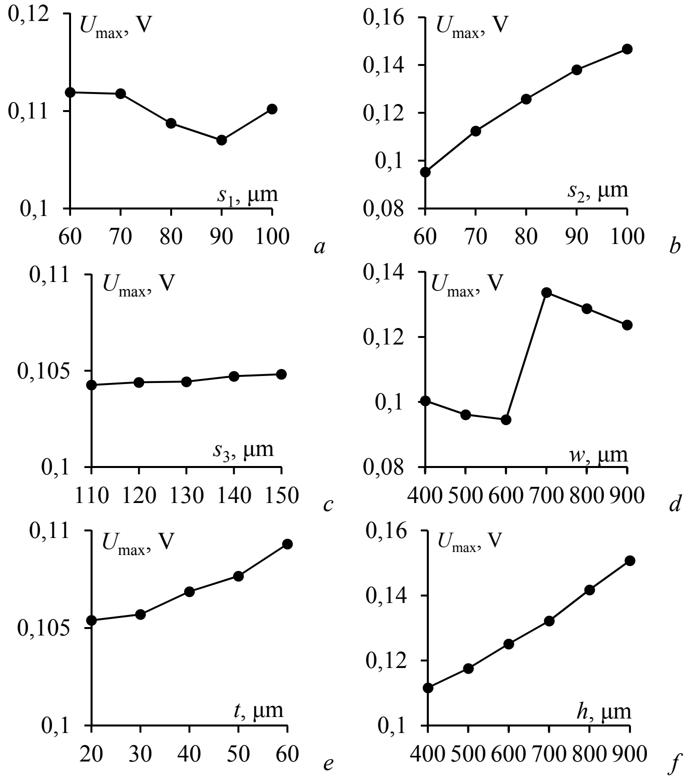

Fig. 4. Dependences of $U_{\max}$ at the end of circuit diagram 2 on s_1 (a), s_2 (b), s_3 (c), w (d), t (e) and h (f).

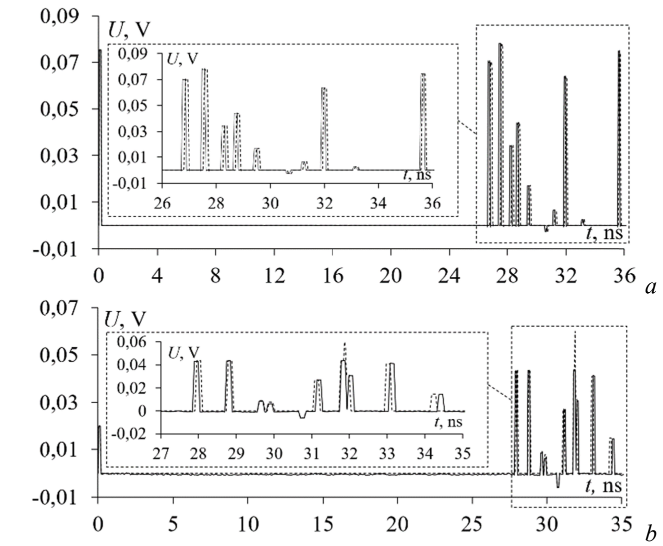

Fig. 5. Voltage waveform obtained in the TALGAT (—) and ADS (---) software at node $V4$ of ciruit 1 (*a*) and $V6$ of ciruit 2 (*b*)

TABLE 3
SETS OF BOUNDARY CONDITIONS (N) OF PASSIVE CONDUCTORS FOR CIRCUIT DIAGRAMS 1 AND 2

	TALGAT		ADS		Deviation, %	
Circuit	1	2	1	2	1	2
t_{P2} [ns]	26.69	27.84	26.76	27.89	0.26	0.18
t_{P3} [ns]	27.43	28.69	27.5	28.70	0.26	0.03
t_{P4} [ns]	28.16	29.55	28.23	29.54	0.25	0.03
t_{P5} [ns]	28.62	29.79	28.68	29.80	0.21	0.03
t_{P6} [ns]	29.35	30.64	29.41	30.63	0.20	0.03
t_{P7} [ns]	30.55	31.08	30.6	31.01	0.16	0.23
t_{P8} [ns]	31.11	31.73	31.17	31.71	0.19	0.06
t_{P9} [ns]	31.84	31.93	31.89	31.83	0.16	0.31
t_{P10} [ns]	33.04	33.03	33.08	32.91	0.12	0.36
t_{P11} [ns]	35.53	34.32	35.56	34.12	0.08	0.59

Fig. 5 shows that the USP at the end of the line under investigation is represented by the sequence of 11 main pulses, the amplitudes of which in the TALGAT software do not exceed 78 mV for circuit 1 (Fig. 5*a*), and 47 mV – for circuit 2 (Fig. 5*b*). Thus, the USP attenuation was 6.4 and 10.6 times (relative to $E/2$) for circuits 1 and 2, respectively. Therefore, the use of circuit 2 is preferable from the point of view of increasing the USP attenuation. From the comparative analysis of the results obtained in the TALGAT and ADS software, it can be seen that the simulation results are in well agreement: almost all pulses agree in amplitude, but there are minor deviations in the delays. Table 3 summarizes the results of comparing the delays (the maximum divergence is 0.6%). Meanwhile, the differences in delays between the decomposition pulses calculated in the TAGAT and ADS software are in good agreement: the maximum deviation does not exceed 80 ps and was found for circuit diagram 2. Fig. 5b shows that the $P8$ and $P9$ pulses are superimposed on each other in the ADS system (due to the small difference in delays between pulses $P8$ and $P9$), which leads to a signal burst with an amplitude of 59 mV. Thus, the obtained results are validated both qualitatively and quantitatively, but in the practical implementation of these devices, it is necessary to pay special attention to the difference in pulses delays.

Based on the results obtained earlier, let us formulate the conditions that allow the decomposition of the USP into 11 pulses in a meander MSL with passive conductors. First, it is necessary to formulate expressions that determine the delays of each pulse of the decomposition. Note that for the line with circuits 1 and 2, the obtained sets of optimal parameters are different; therefore, the sequence of decomposition pulses will be different (in Fig. 2*d* pulses $P7$ and $P8$ are swapped). Considering this, in the circuit 1, the pulse delays are defined as: $t_{P2}=2l\tau_1$, $t_{P3}=l\tau_1+l\tau_2$, $t_{P4}=2l\tau_2$, $t_{P5}=l\tau_1+l\tau_3$, $t_{P6}=l\tau_2+l\tau_3$, $t_{P7}=2l\tau_3$, $t_{P8}=l\tau_1+l\tau_4$, $t_{P9}=l\tau_2+l\tau_4$, $t_{P10}=l\tau_3+l\tau_4$, $t_{P11}=2l\tau_4$. The delays of $P2$–$P6$ and $P9$–$P11$ pulses in the circuit 2 are determined similarly; however, the pulses $P7$ and $P8$ are swapped so that: $t_{P7}=l\tau_1+l\tau_4$ and $t_{P8}=2l\tau_3$. Knowing the expressions that determine the delays of each of the 10 decomposition pulses (except for the first one, which arrives without delay and is induced), it is possible to ensure the USP decomposition by fulfilling a number of conditions, similarly to the way it has been done in [15]. However, these conditions will be different for lines with circuits 1 and 2, since pulses $P7$ and $P8$ have different arrival times. Then, the conditions for the decomposition of the USP in the circuit 1:

$$2l\tau_1 \geq t_{USP}, \tag{1}$$

$$l\tau_2 \geq l\tau_1+t_{USP}, \tag{2}$$

$$l\tau_1+l\tau_3 \geq 2l\tau_2+t_{USP}, \tag{3}$$

$$l\tau_3 \geq l\tau_2+t_{USP}, \tag{4}$$

$$l\tau_1+l\tau_4 \geq 2l\tau_3+t_{USP}, \tag{5}$$

$$l\tau_4 \geq l\tau_3+t_{USP} \tag{6}$$

where l is the length of a transmission line segment and t_{USP} is the total USP duration time. The conditions for the USP decomposition in the line with circuit 2 are the same as (1)–(3), (4) and (6), while instead of (5) the following two conditions must be met:

$$l\tau_1+l\tau_4 \geq l\tau_2+l\tau_3+t_{USP}, \tag{7}$$

$$2l\tau_3 \geq l\tau_1+l\tau_4+t_{USP}. \tag{8}$$

Conditions (1)–(6) for the circuit 1 and (1)–(3), (4), (6)–(8) for the line with the circuit 2 and with the previously found optimal parameters were checked. For this, we first calculated the per-unit-length delays of the modes in the TALGAT software of the line under investigation. For the first parameter set they were τ_1=11.12 ns/m, τ_2=11.73 ns/m τ_3=12.72 ns/m, τ_4=14.8 ns/m, and for the second, they were τ_1=11.6 ns/m, τ_2=12.31 ns/m τ_3=13.22 ns/m, τ_4=14.29 ns/m. Based on the per-unit-length delays, the delays of each of the 10 decomposition pulses in the TALGAT software were calculated. For the circuit 1, they were t_{P2}=26.69 ns, t_{P3}=27.42 ns, t_{P4}=28.16 ns, t_{P5}=28.62 ns, t_{P6}=29.35 ns, t_{P7}=30.55 ns, t_{P8}=31.11 ns, t_{P9}=31.84 ns, t_{P10}=33.04 ns, t_{P11}=35.53 ns, and for the line with circuit 2 they were t_{P2}=27.82 ns, t_{P3}=28.68 ns, t_{P4}=29.54 ns, t_{P5}=29.80 ns, t_{P6}=30.63 ns, t_{P7}=31.07 ns, t_{P8}=31.72 ns, t_{P9}=31.92 ns, t_{P10}=33.02 ns, t_{P11}=34.31 ns. Thus, when the known values are substituted into expressions (1)–(8), the conditions for the line with circuits 1 and 2 are fulfilled: the delay of each pulse is not less than the sum of the delays of the previous one and the total USP duration.

IV. CONCLUSION

The paper considered the decomposition of a USP in a turn of a meander MSL with two passive conductors into a sequence of pulses of lower amplitude. Two circuit diagrams were considered. Various boundary conditions of the passive conductors were considered and the optimal parameters were obtained according to the criterion of the minimum amplitude at the output. Moreover, we analyzed the influence of the geometric parameters of the line under investigation on the delays of each decomposition pulse and USP amplitude at the end of the turn and formulated the conditions for USP decomposition. The optimal parameters of the investigated line were found, which ensure USP decomposition and the minimization of its amplitude. The attenuation of the USP (relative to half of the e.m.f.) for the optimal parameters in the first circuit was 6.4 times, and in the second – 10.6 times.

It is important to note that the sets of optimal parameters obtained in this paper by heuristic search do not determine the global minimum value of the output signal amplitude. In addition, the decomposition conditions can change if the sequence of pulse arrivals changes. Therefore, to find the global minimum, it is advisable to use evolutionary methods, for example, genetic algorithms. This seems promising for further investigation.

ACKNOWLEDGMENT

The research was supported by the Russian Scientific Foundation, project 21-79-00161 (simulation) and Ministry of Science and Higher Education of the Russian Federation, project FEWM-2022-0001 (models).

REFERENCES

[1] T.R. Gazizov, *Electromagnitnyi terrorizm na rubezhe tysyacheletiy* [Electromagnetic Terrorism at the Turn of the Millennium], Tomsk State University, Tomsk, 2002, pp. 204. (in Russian).

[2] E.N. Fominich and D.R. Vladimirov, "Elektromagnitnyj terrorizm. Novaya ugroza dlya informacionno-upravlyayushchih sistem [Electromagnetic terrorism. A new threat to management information systems]", *Voennyj inzhener*, vol. 2, no. 2, 2016, pp. 10-17. (in Russian).

[3] O. Petkau, A. Tarabtsev, A. Deryabin, S. Larionov, and V. Chvanov, "Protection of the Fuel and Energy Complex Against Electromagnetic Threats", Bezopasnost ob'ektov toplivno-energeticheskogo kompleksa [Safety of objects of the fuel and energy complex], vol. 2, no. 6, pp. 74-76, 2014. (in Russian)

[4] C. Mojert, D. Nitsch, H. Friedhoff, J. Maack, F. Sabath, M. Camp, and H. Garbe, "UWB and EMP Susceptiblity of Microprocessors and Networks", *14th International Zurich Symposium on EMC*, Zurich, Switzerland, February 20-22, 2001, pp. 47-52.

[5] Z.M. Gizatullin and R.M. Gizatullin, "Investigation of the Immunity of Computer Equipment to the Power-Line Electromagnetic Interference", *Journal of Communications Technology and Electronics*, vol. 61, 2016, pp. 546-550, 10.1134/S1064226916050053.

[6] S.A. Zajkova, *Passivnye komponenty radioelektronnoj apparatury* [Passive components of electronic equipment], Posobie, Grodno: GrGU, 2009, p. 67. (in Russian).

[7] A.S. Koldunov, *Radiolyubitel'skaya azbuka. Analogovye ustrojstva* [Radio alphabet. Analog devices], M: Solon-Press, vol. 2, 2004, p. 288. (in Russian).

[8] R. Krzikalla, J. Luiken, L. ter Haseborg, and F. Sabath, "Systematic Description of the Protection Capability of Protection Elements", *2007 IEEE International Symposium on Electromagnetic Compatibility*, Honolulu, HI, USA, 2007, pp. 1-5, doi: 10.1109/ISEMC.2007.177.

[9] R. Krzikalla, T. Weber, and J.L. ter Haseborg, "Interdigital Microstrip Filters as Protection Devices Against Ultrawideband Pulses", *2003 IEEE International Symposium on Electromagnetic Compatibility*, Istanbul, Turkey, 2003, vol. 2, pp. 1313-1316, doi: 10.1109/ICSMC2.2003.1429162.

[10] R. Krzikalla and J.L. ter Haseborg, "SPICE Simulations of UWB Pulse Stressed Protection Elements Against Transient Interferences", *2005 IEEE International Symposium on Electromagnetic Compatibility*, Chicago, IL, USA, 2005, vol. 3, pp. 977-981, doi: 10.1109/ISEMC.2005.1513667.

[11] T. Webe, R. Krzikalla, and J.L. ter Haseborg, "Linear and Nonlinear Filters suppressing UWB Pulses", *IEEE Transactions on Electromagnetic Compatibility*, vol. 46, no. 3, August 2004, pp. 423-430, doi: 10.1109/TEMC.2004.831887.

[12] Q. Cui, S. Dong, and Y. Han, "Investigation of Waffle Structure SCR for Electrostatic Discharge (ESD) Protection", *2012 IEEE International Conference on Electron Devices and Solid State Circuit (EDSSC)*, Bangkok, Thailand, December 2012, pp. 1-4, doi: 10.1109/EDSSC.2012.6482791.

[13] H. Hayashi, T. Kuroda, K. Kato, K. Fukuda, S. Baba, and Y. Fukuda, "ESD Protection Design optimization Using a Mixed-Mode Simulation and its Impact on ESD Protection Design of Power Bus Line Resistance", *2005 International Conference on Simulation of Semiconductor Processes and Devices (SISPAD 2005)*, Tokyo, Japan, September 2005, pp. 99-102, doi: 10.1109/SISPAD.2005.201482.

[14] A.V. Nosov, "Sovershenstvovanie zashchity radioelektronnoj apparatury ot sverhkorotkih impul'sov za schet meandrovyh linij zaderzhki [Improving the Protection of Radio Electronic Equipment from ultrashort Pulses Using Meander Delay Lines]", Ph.D. dissertation, Dept. Telev. and Cont., Tomsk State Univ. of Cont. Sys. and Radioelec., Tomsk, RF, 2018, pp. 185. (in Russian).

[15] A.O. Belousov, E.B. Chernikova, M.A. Samoylichenko, A.V. Medvedev, A.V. Nosov, T.R. Gazizov and A.M. Zabolotsky, "From Symmetry to Asymmetry: The Use of Additional Pulses to Improve Protection Against Ultrashort Pulses Based on Modal Filtration", *Symmetry*, vol. 12, no. 7, Article ID 1117, pp. 1-39, 2020, doi: 10.3390/sym12071117.

[16] A.V. Nosov and R.S. Surovtsev, "Ultrashort Pulse Decomposition in the turn of a Meander Microstrip Line with a Passive Conductor", *Journal of Physics: Conference Series (JPCS)*, 2021, vol. 1862, no. 1, pp. 1-6, doi: 10.1088/1742-6596/1862/1/012029.

[17] S.P. Kuksenko, "Preliminary Results of TUSUR University Project for Design of Spacecraft Power Distribution Network: EMC Simulation", *IOP Conference Series: Materials Science and Engineering*, vol. 560, pp. 1-7, 2019, doi: 10.1088/1757-899X/560/1/012110.

[18] Certificate of state registration of a computer program No. 2018611481. TALGAT 2017. Application No. 2017663209. Date of receipt December 13, 2017 Registered in the Register of computer programs 02.02.2018.